RESEARCH

Investigation of ZnO thin-film sensing properties for CO_2 detection: effect of Mn doping

Boshra Ghanbari Shohany[1] · Leili Motevalizadeh[2] · Majid Ebrahimizadeh Abrishami[1]

Abstract

A simple spray pyrolysis technique has been used to fabricate ZnO/Mn thin films with different Mn concentrations (0, 5, 10 and 15 mol.%) for gas sensing applications. X-ray diffraction (with Cu-Kα radiation) patterns of the samples revealed the formation of single-phase wurtzite structure. The samples were characterized using field-emission scanning electron microscopy and scanning tunneling microscopy. The investigation revealed that the surface of pure ZnO thin film appears rougher and containing bigger grains. The response of the pure and Mn-doped ZnO thin-film gas sensors was checked at different temperatures ranging from 120 up to 200 °C, to investigate the optimum sensing efficiency. The gas sensing results have demonstrated that the pure ZnO thin film exhibited higher sensitivity to CO_2 gas at 150 °C operating temperature, while the sensitivity reduced with the increase in gas pressure. Although the sensitivity of doped samples was lower than the pure sample, the sensitivity increased with the increase in pressure.

Keywords ZnO/Mn · Sensing properties · CO_2 gas · Thin films

Introduction

Zinc oxide (ZnO) has given a great deal of attention due to large exciton binding energy (60 meV) and large direct band gap energy (3.37 eV) at room temperature [1–3]. ZnO is widely used in various applications such as transistors, piezoelectric devices, solar cell electrodes and gas sensors. ZnO is sensitive to many gases such as CO [4–6], O_2 [7–9], CH_4 [10–12], NO_2 [13–15] and ethanol [16–18], due to its well-known surface conductivity.

In the past few years, many efforts have been devoted to improve the sensitivity of gas sensors. Gas sensing properties are dependent on structure, morphology, grain size and surface area of the sensing materials. As an interesting chemically and thermally stable *n*-type semiconductor, ZnO-based gas sensors have been studied experimentally and theoretically in order to investigate the relation between the sensitivity and the microstructure of zinc oxide for gas sensors [19–21]. The grain size is one of the most important factors affecting sensing properties. Dong et al. showed that nano-ZnO exhibits higher sensitivity and lower operating temperatures compared to coarse-grained ZnO. Their results showed that the smaller grain size of pure ZnO has higher gas sensitivity [22]. Chang et al. fabricated ZnO films with variable thickness (65–390 nm) using RF reactive sputtering. The effect of film thickness on sensing properties was investigated. The thinnest film exhibits the best sensitivity and fastest response [23]. Eriksson et al. used resistive sensor measurements with respect to oxygen sensitivity in order to characterize sensing layers based on ZnO nanoparticles and films. The ZnO nanoparticles showed a better response to oxygen as compared to the films. The higher sensitivity was ascribed to a larger surface-to-volume ratio, and the higher stability to the generally more stable single-crystalline nanoparticles [9].

✉ Boshra Ghanbari Shohany
   boshrags@yahoo.com

✉ Leili Motevalizadeh
   lmotevali@mshdiau.ac.ir; lmotevali@yahoo.com

   Majid Ebrahimizadeh Abrishami
   ebrahimizadeh@ymail.com

1 Department of Physics, Ferdowsi University of Mashhad, Mashhad, Iran

2 Department of Physics, Mashhad Branch, Islamic Azad University, Mashhad, Iran

Ⓐ Springer

The major drawbacks of ZnO-based gas sensors are the poor sensitivity and high operating temperature (approximately 400 °C). Doping of metal oxide sensing film is a traditional technology for gas sensors. The traditional concept of doping is to enhance catalytic activity and adjust electrical resistance of the intrinsic metal oxide [24]. Doping ZnO with various element was used to enhance the sensing properties and reduce the operating temperature of zinc oxide-based gas sensors. Lupan et al. were prepared ZnO and ZnO/Al thin films by chemical solution deposition and photo-thermal processing techniques. Their results showed that the morphological, electrical and sensing properties of zinc oxide films can be modified by controlling the growth regimes and doping concentration. Nanostructured ZnO/Al showed a higher sensitivity to CO_2 gas compared to undoped ZnO films [25]. Gaspera et al. investigated the effect of doping with transition metal ions on the CO optical sensing properties of nanocrystalline ZnO films. Transition metal ions inside the ZnO lattice structure were found to increase the magnitude of the response and the sensitivity of the nanocomposites [26]. Al-Hardan et al. synthesized Cr-doped ZnO thin films by RF reactive co-sputtering. The operating temperature of the Cr-doping ZnO gas sensor was shifted to lower temperature (around 250 °C). The response to oxygen gas was enhanced by doping ZnO with Cr [7]. Hu et al. used the transition metals as dopants for the synthesis of ZnO nanorods by plasma-enhanced chemical vapor deposition (PECVD) method. The doped ZnO nanorods showed the superior formaldehyde sensing property in a few second response and recovery time [27].

We recently reported the electrical properties of Mn-doped zinc oxide thin films with different amounts of Mn concentrations by a spray pyrolysis technique [28]. In the following, this study discusses the effect of Mn doping on the sensing properties of ZnO thin films in the presence of carbon dioxide gas. Our result showed that the best sensing parameter is obtained in pure ZnO film.

Methods

The precursors used for the synthesis of ZnO/Mn thin films with different amounts of Mn concentrations (0, 5, 10 and 15 mol.%) were Zinc acetate, manganese acetate, isopropanol, acetic acid and distilled water. ZnO/Mn thin films were fabricated by the parameters previously reported in Refs. [28, 29] using the spray pyrolysis technique.

The crystallite phase of the samples was characterized by X-ray diffraction (XRD) using Cu-Kα radiation. For structural characterization, analysis of the obtained XRD profile was performed using the Rietveld refinement method, through the Fullprof software. The crystallite size

(D) was estimated using Scherrer's equation, and the element composition of all thin films was detected by energy-dispersive X-ray spectroscopy (EDS). The surface morphology and topography of the samples were analyzed by using field-emission scanning electron microscopy (FESEM) at 30 kV and scanning tunneling microscopy (STM). The thickness of the films was measured by using the laser ellipsometer (SENTECH, SE500adv CER—Germany).

In order to characterize the gas sensing properties of Mn-doped ZnO thin films, Al electrodes were deposited by thermal evaporation at the pressure of 10^{-6} torr and a setup was used as schematically shown in Fig. 1. The sample was placed in a sealed chamber, and the resistivity of the sample in the presence of CO_2 gas was measured. The resistance response of each sample was transformed into a sensitivity value using the following formula:

$$S = \left| (R_{\text{gas}} - R_0)/R_0 \right| \tag{1}$$

where R_{gas} is the resistance of the film influenced by the gas and R_0 is the resistance of the film in the air [30].

Results and discussions

Results of X-ray diffraction revealed the formation of approximately single-phase materials for pure and all Mn-doped thin films. They crystallize in the characteristic wurtzite structure. A Rietveld refined pattern of a typical sample with 15 mol.% Mn-doped layer is presented in Fig. 2, and the results of the structural data are presented in Table 1. The lattice parameters of the thin films were very close, and the average crystalline size of the ZnO/Mn thin films was observed to be less than the undoped ZnO film.

Two typical EDS spectra of the doped layer with 5 and 15 mol.% Mn are shown in Fig. 3. The presence of the constituent elements for Mn-doped ZnO, Zn, O and Mn were confirmed by the occurrence of their respective peaks. The other peaks Ca and Si presented the composition of glass substrate, and Au peaks are from the gold coating.

Figure 4 shows the FESEM images of the pure and Mn-doped ZnO thin films grown at 500 °C on glass substrates. As can be seen in this figure, the pure ZnO thin film has rougher surface than Mn-doped ZnO and by increasing the Mn concentration to 10 mol.%, the roughness decreases. But with the increase in Mn concentration to 15 mol.%, Mn oxide was agglomerated and created bright clusters, as shown in FESEM image. Therefore, based on the analysis of FESEM images, the solubility limit of Mn in our samples is 10 mol.%.

Figure 5 shows the 3D-STM images of the pure and 5 mol.% Mn-doped ZnO thin films. The surface morphology of the thin films indicates that the surface of pure ZnO

Fig. 1 Setup for measurement of sensing properties of Mn-doped ZnO films as CO_2 gas sensor
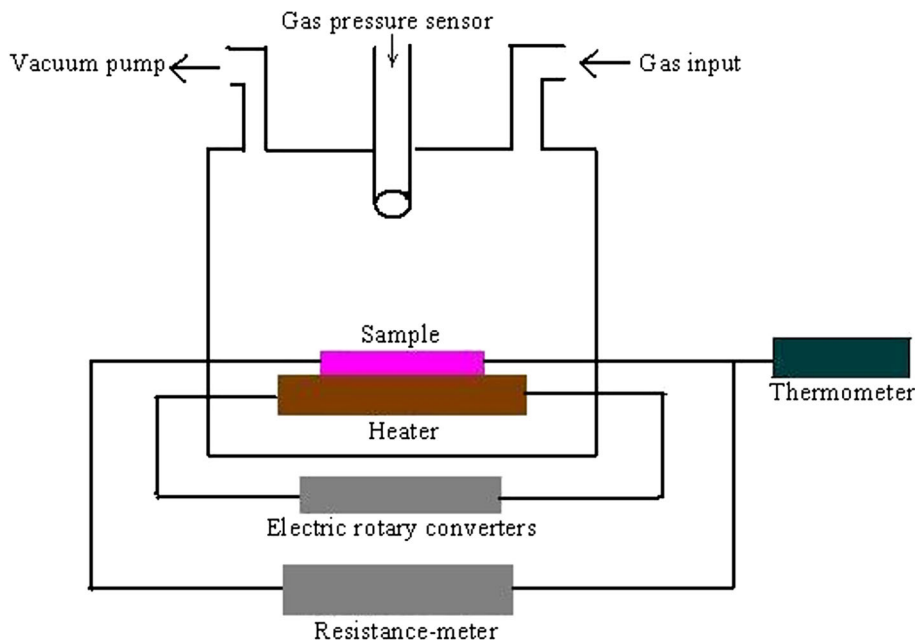
Fig. 2 A Rietveld refined pattern of a typical sample with 15 mol.% Mn-doped layer. The observed (circles) and calculated (solid lines) patterns are shown. The vertical bars indicate the position of Bragg reflections. The difference between the observed and calculated intensities is given at the bottom of the diagram
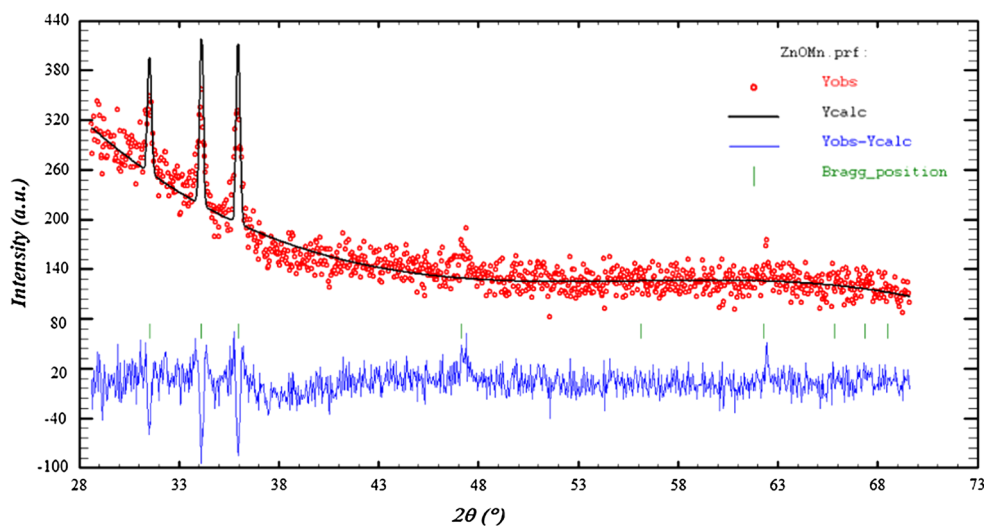
Table 1 Lattice constants and crystalline size measured by XRD data, the thickness of the films estimated by ellipsometry technique

Mn content (mol.%)	a (Å)	c (Å)	V (Å)	Crystalline size (nm)	Film thickness (nm)
0	3.2400	5.1750	54.3251	31.5	252
5	3.2440	5.1768	54.4782	23.5	281
10	3.2432	5.1765	54.4482	24.7	300
15	3.2430	5.1760	54.4362	25.5	311

appears rougher and containing bigger grains (as seen in FESEM images).

The variations of sensitivity obtained for pure ZnO and ZnO/Mn 5 mol.% thin films as a function of temperature at different pressures of CO_2 gas ($P = 100$, 200 and 300 torr) are shown in Figs. 6 and 7, respectively. As shown in Fig. 6, the sensitivity of the ZnO film monotonically increases with the increase in temperature, while the sensitivity decreases with the increase in pressure.

As seen in Fig. 7, the isopressure curves of the sensitivity of ZnO/Mn 5 mol.% increase exponentially with the increase in the temperature. However, the upward trend of sensitivity with the increase in the pressure from 100 to
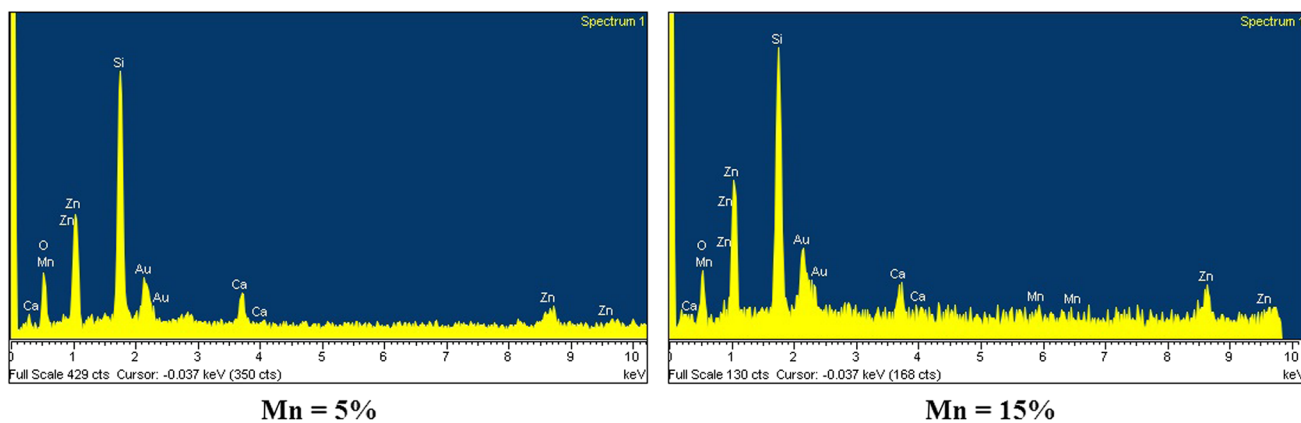
Fig. 3 EDS spectra of the doped layer with 5 and 15 mol.% Mn
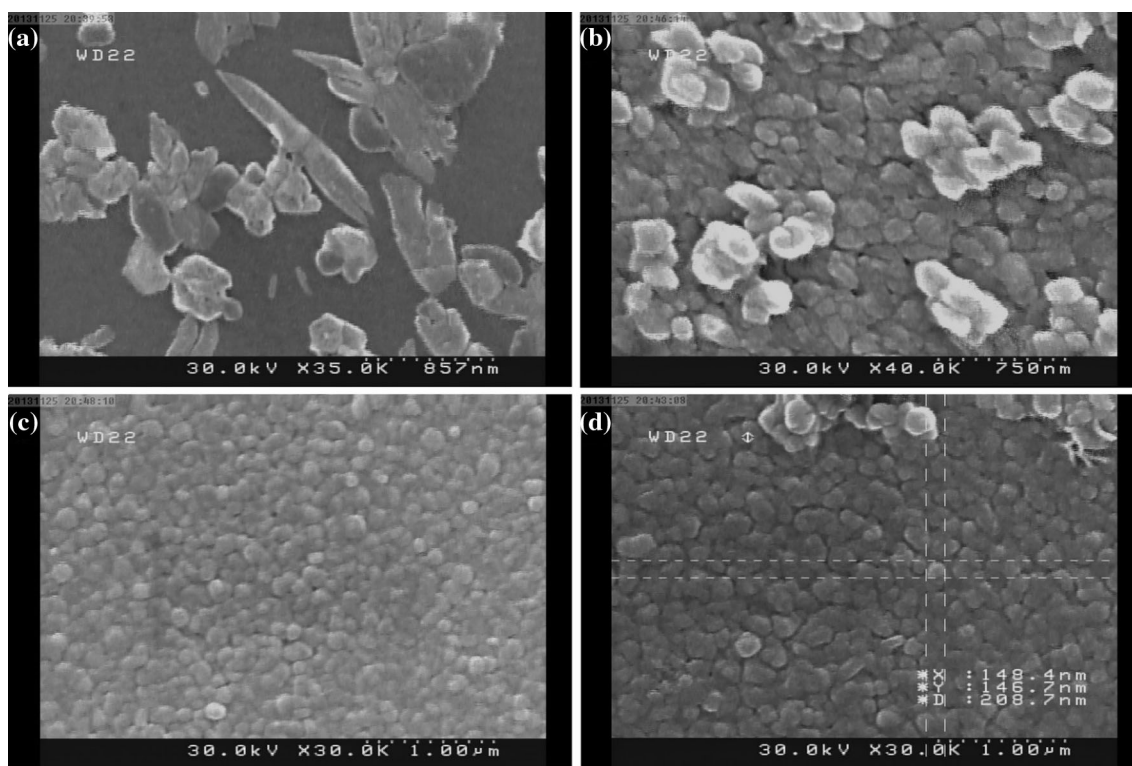

Fig. 4 FESEM images of ZnO/Mn thin films. **a** Mn: 0.0 mol.%, **b** Mn: 5.0 mol.%, **c** Mn: 10.0 mol.% and **d** Mn: 15.0 mol.%

300 torr is not consistent with the trend observed for undoped ZnO thin film.

Figure 8 shows the sensitivity of the all samples as a function of CO_2 gas pressure measured at 150 °C. As it is shown, by Mn doping in ZnO, sensing properties of thin films considerably decreased. Also it can be seen, by increasing the pressure of CO_2 gas into the test chamber, the sensitivity decreased in pure ZnO, but increased in ZnO/Mn.

Thickness of the films measured by ellipsometry technique is given in Table 1. As it shows the thickness of the films is not the same and the Mn-doped layer is thicker than the pure one. The curves of the sensitivity of all samples versus the thickness of films measured at 150 °C and 300 torr are shown in Fig. 9. It can be seen by increasing the thickness, the sensitivity of the films decreased. It is clear because the sensitivity is the reciprocal of resistivity and the resistivity of the films increases by thickness [23, 28].

The performance of gas sensors is considerably influenced by different parameters such as structure of sensing materials, particle size, grain boundaries, doping atoms,
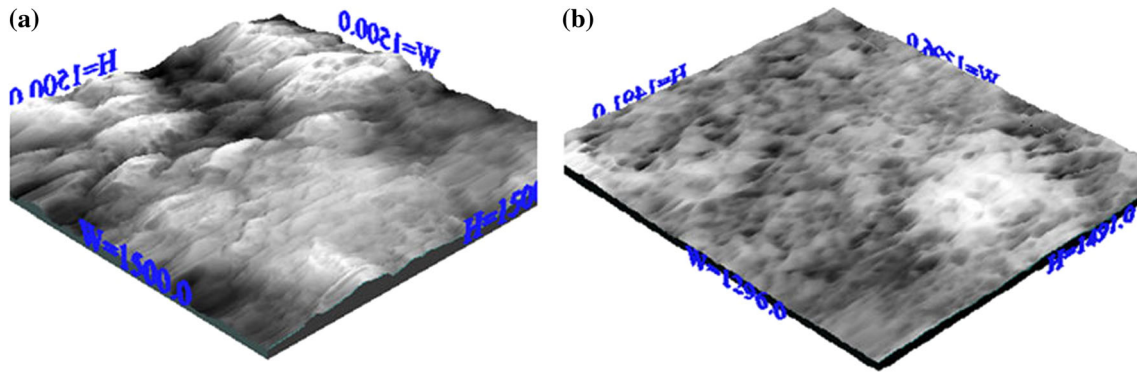
Fig. 5 3D-STM images from the surface of **a** Pure ZnO and **b** ZnO/Mn 5 mol.% thin films
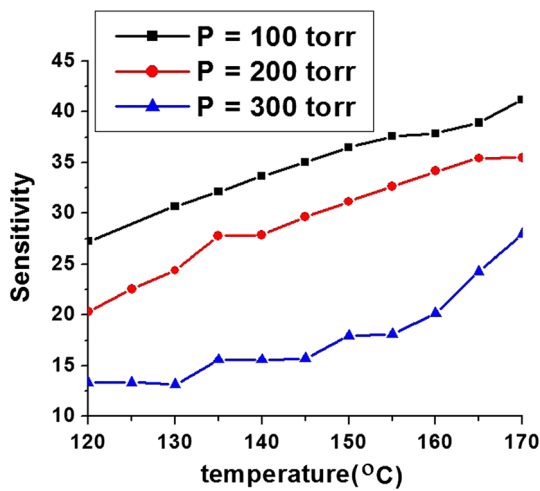

Fig. 6 Variation of sensitivity for pure ZnO layer as a function of temperature at different pressures of CO_2 gas (P = 100, 200 and 300 torr)

Fig. 8 Sensitivity of ZnO/Mn thin films with different Mn concentrations as a function of CO_2 gas pressure measured at 150 °C
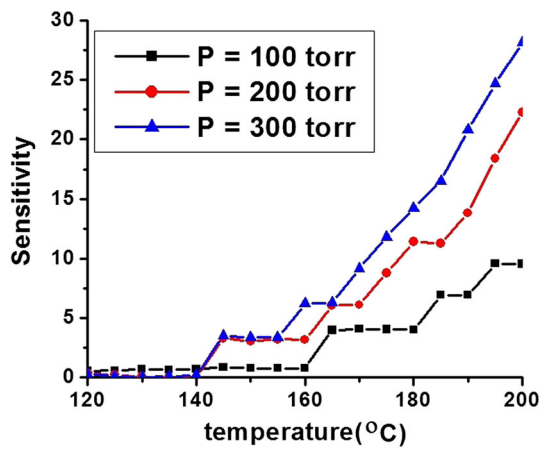

Fig. 7 Variation of sensitivity for ZnO/Mn 5 mol.% as a function of temperature at different pressures of CO_2 gas (P = 100, 200 and 300 torr)
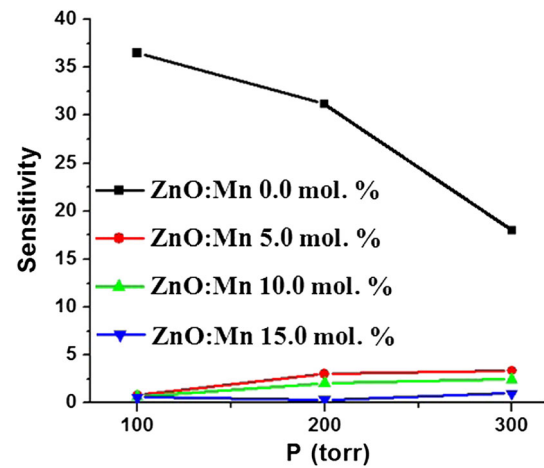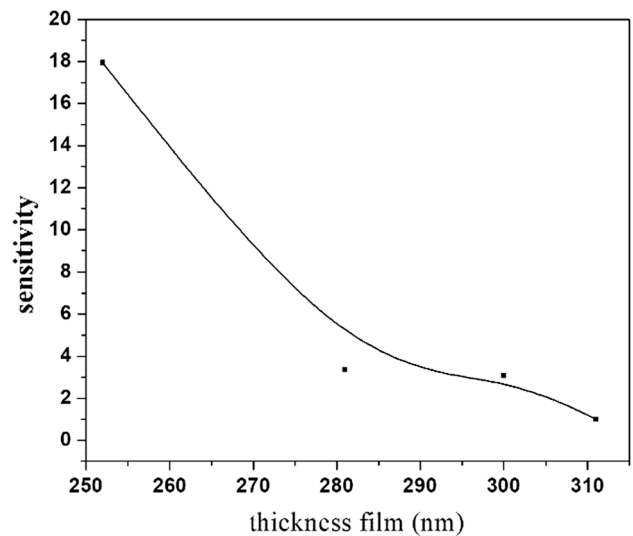

Fig. 9 Sensitivity of ZnO/Mn versus the thickness of films measured at 150 °C and 300 torr

porosity and morphology of films. The sensing mechanism of *n*-type metal oxide gas sensors such as ZnO is given below.

Oxygen species can capture the electrons from the inner layer of ZnO films. Therefore, the oxygen species adsorbed and consequently the negative charges of the film would be trapped. The trapping of electrons causes an upward band bending and thus a decrease in conductivity comparing to the flat band situation [31].

In the presence of a deoxidizing gas, the electrons trapped by the oxygen adsorbate return to the ZnO film and lead to decrease in the potential barrier height and increase in conductivity. So the oxygen vacancies act as donors and increase the surface conductivity. There are different kinds of oxygen species in the gas phase including molecular (O_2^-) and atomic (O^-, O^{2-}) ions, adsorbed at the surface of ZnO films. On the surface of ZnO thin films, the reaction $O_{2ads}^- + e^- = 2O_{ads}^-$ takes place as the temperature increases. The desorption temperature is around 150 °C for O_{2ads}^- and greater for O_{ads}^- [31–33]. When the sensor is exposed to air, the oxygen molecules may capture the electrons and lead to increase the resistance, whereas by exposing the reductive gas to the samples, the absorbed oxygen ions react with the target gas, so the trapped electrons move back to the conduction band and the resistance decreases [34]. According to the mechanism explained above, we can discuss about the behavior of our samples.

As Fig. 6 shows the sensor response of pure ZnO thin film increases gradually versus the temperature, cause for operating temperatures < 200 °C, the adsorbed CO_2 molecules are not activated enough to react with the surface adsorbed oxygen species [35], whereas the significant enhancement in the response of the Mn-doped ZnO thin films to CO_2 gas by increasing temperature as seen in Fig. 7 can be attributed to the decrease in the contact resistance between the grains [36]. Generally with increasing Mn concentration, carrier density decreases; moreover, the Mn atoms prefer to be accumulated in the grain boundaries and contribute to the oxidation process and consequently the oxygen deficiencies decrease. So the presence of Mn in ZnO films increases the resistance due to decrease in the oxygen deficiencies and accumulation of Mn atoms in the grain boundaries [28]. In the other hand, the incorporation of substitutional Mn suppresses the formation of native defects such as oxygen vacancies. Therefore by CO_2 exposing to these samples, their resistivity does not change so much and consequently the sensitivity of the doped samples is not considerable as shown in Figs. 7 and 8. The roughness of the films is the other parameter which affects the sensitivity. By analysis of FESEM and STM images, the roughness decreased and oxygen deficiency reduced as said before. Also increasing

the thickness of Mn-doped layers caused the sensitivity of the films decreased. Therefore, sensing parameter of ZnO/Mn thin film decreased comparing to the undoped sample. Decreasing the sensitivity of the pure ZnO thin film by increasing the pressure in Fig. 8 causes to lower tendency of absorbing oxygen species by increasing concentration of CO_2 gas.

Comparison between our results with other researches indicates that the pure ZnO thin film synthesized by this method has a good sensing properties at relatively low operating temperature [25, 37, 38].

Conclusion

Zinc oxide thin films with different Mn concentrations (0, 5, 10 and 15 mol.%) has been deposited via spray pyrolysis technique. The FESEM and 3D-STM images of the thin films indicate that the surface of pure ZnO is rougher than ZnO/Mn and containing bigger grains. The variations of sensitivity as a function of temperature at different pressures of CO_2 gas have been investigated. The results showed that by increasing the temperature, the sensitivity of the all samples increased and by Mn doping in ZnO, sensing properties of thin films considerably decreased. Also by increasing concentration of CO_2 gas, the sensitivity of ZnO/Mn did not change so much, but the sensitivity of the pure ZnO thin film decreased due to lower tendency of absorbing oxygen species.

References

1. Chen, Y., Bagnall, D.M., Koh, H.-J., Park, K.-T., Hiraga, K., Zhu, Z.-Q., TJ, Yao: Plasma assisted molecular beam epitaxy of ZnO on c-plane sapphire: Growth and characterization. Appl. Phys. **84**, 3912 (1998)
2. Srikant, V., Clarke, D.R.: On the optical band gap of zinc oxide. J. Appl. Phys. **83**, 5447 (1998)
3. Liu, M., Kim, H.K.: Ultraviolet detection with ultrathin ZnO epitaxial films treated with oxygen plasma. Appl. Phys. Lett. **84**, 173 (2004)
4. Chang, S.J., Hsueh, T.J., Chen, I.C., Huang, B.R.: Highly sensitive ZnO nanowire CO sensors with the adsorption of Au nanoparticles. Nanotechnology **19**, 175502 (2008)
5. Wang, J.X., Sun, X.W., Yang, Y., Huang, H., Lee, Y.C., Tan, O.K., Vayssieres, L.: Hydrothermally grown oriented ZnO nanorod arrays for gas sensing applications. Nanotechnology **17**, 4995 (2006)

6. Bârsan, N., Weimar, U.: Understanding the fundamental principles of metal oxide based gas sensors; the example of CO sensing with SnO_2 sensors in the presence of humidity. J. Phys. Condens. Matter **15**, R813 (2003)

7. Al-Hardan, N., Abdullah, M.J., Abdul Aziz, A.: Impedance spectroscopy of undoped and Cr-doped ZnO gas sensors under different oxygen concentrations. Appl. Surf. Sci. **257**, 8993 (2011)

8. Eriksson, J., Khranovskyy, V., Söderlind, F., Käll, P., Yakimova, R., Lloyd-Spets, A.: ZnO nanoparticles or ZnO films: a comparison of the gas sensing capabilities. Sens. Actuators B **137**, 94 (2009)

9. Lu, C.Y., Chang, S.P., Chang, S.J., Hsueh, T.J., Hsu, C.L., Chiou, Y.Z., Chen, I.C.: ZnO nanowire-based oxygen gas sensor. IEEE Sens. J. **9**, 485 (2009)

10. Hamedani, N.F., Mahjoub, A.R., Khodadadi, A.A., Mortazavi, Y.: CeO_2 doped ZnO flower-like nanostructure sensor selective to ethanol in presence of CO and CH4. Sens. Actuators B **169**, 67 (2012)

11. Hamedani, N.F., Mahjoub, A.R., Khodadadi, A.A., Mortazavi, Y.: Microwave assisted fast synthesis of various ZnO morphologies for selective detection of CO, CH_4 and ethanol. Sens. Actuators B **156**, 737 (2011)

12. Mahmoud, F.A., Kiriakidis, G.: Nanocrystalline ZnO thin film for gas sensor application. J. Ovonic Res. **5**, 15 (2009)

13. Park, J., Oh, J.Y.: Highly-sensitive NO_2 detection of ZnO nanorods grown by a sonochemical process. J. Korean Phys. Soc. **55**, 1119 (2009)

14. Shishiyanu, S.T., Shishiyanu, T.S., Lupan, O.I.: Sensing characteristics of tin-doped ZnO thin films as NO_2 gas sensor. Sens. Actuators B Chem. **107**, 379 (2005)

15. Ahn, M.W., Park, K.S., Heo, J.H., Park, J.G., Kim, D.W., Choi, K.J., Lee, J.H., Hong, S.H.: Gas sensing properties of defect-controlled ZnO-nanowire gas sensor. Appl. Phys. Lett. **93**, 10.1063 (2008)

16. Pandya, H.J., Chandra, S., Vyas, A.L.: Integration of ZnO nanostructures with MEMS for ethanol sensors. Sens. Actuators B **161**, 923 (2012)

17. Chen, H., Liu, Y., Xie, C., Wu, J., Zeng, D., Liao, Y.: A comparative study on UV light activated porous TiO_2 and ZnO film sensors for gas sensing at room temperature. Ceram. Int. **38**, 503 (2012)

18. Wan, Q., Li, Q.H., Chen, Y.J., Wang, T.H., He, X.L., Li, J.P., Lin, C.L.: Fabrication and ethanol sensing characteristics of ZnO nanowire gas sensors. Appl. Phys. Lett. **84**, 3654 (2004)

19. Krishnakumar, T., Jayaprakash, R., Pinna, N., Donato, N., Bonavita, A., Micali, G., Neri, G.: CO gas sensing of ZnO nanostructures synthesized by an assisted microwave wet chemical rout. Sens. Actuators B **143**, 198 (2009)

20. Kim, K., Song, Y.W., Chang, S., Kim, I.H., Kim, S., Lee, S.Y.: Fabrication and characterization of Ga-doped ZnO nanowire gas sensor for the detection of CO. Thin Solid Films **518**, 1190 (2009)

21. Xu, J., Pan, Q., Shun, Y., Tian, Z.: Grain size control and gas sensing properties of ZnO gas sensor. Sens. Actuators B **66**, 277 (2000)

22. Dong, L.F., Cui, Z.L., Zhang, Z.K.: Gas sensing properties of nano-ZnO prepared by arc plasma method. Nano Struct. Mater. **8**, 815 (1997)

23. Chang, J.F., Kuo, H.H., Leu, I.C., Hon, M.H.: The effects of thickness and operation temperature on ZnO:Al thin film CO gas sensor. Sens. Actuators B **84**, 258 (2002)

24. Zhu, B.L., Xie, C.S., Wang, W.Y., Huang, K.J., Hu, J.H.: Improvement in gas sensitivity of ZnO thick film to volatile organic compounds (VOCs) by adding TiO_2. Mater. Lett. **58**, 624 (2004)

25. Lupan, O., Chow, L., Shishiyanu, S., Monaico, E., Shishiyanu, T., Şontea, V., Roldan Cuenya, B., Naitabdi, A., Park, S., Schulte, A.: Nanostructured zinc oxide films synthesized by successive chemical solution deposition for gas sensor applications. Mater. Res. Bull. **44**, 63 (2009)

26. Gaspera, E.D., Guglielmi, M., Perotto, G., Agnoli, S., Granozzi, G., Post, M.L., Martucci, A.: CO optical sensing properties of nanocrystalline ZnO–Au films: effect of doping with transition metal ions. Sens. Actuators B Chem. **161**, 675 (2012)

27. Hu, P., Han, N., Zhang, D., Ho, J.C., Chen, Y.: Highly formaldehyde-sensitive, transition-metal doped ZnO nanorods prepared by plasma-enhanced chemical vapor deposition. Sens. Actuators B **169**, 74 (2012)

28. Motevalizadeh, L., Ghanbari Shohany, B., Abrishami, M.E.: Effects of Mn doping on electrical properties of ZnO thin films. Mod. Phys. Lett. B **30**, 1650024 (2016)

29. Abrishami, M.E.: Carrier density dependence of sp-d exchange in nanostructured ZnO:Mn thin film. In: Proceedings of the International Conference Nanomaterials: Applications and Properties, vol. 1, p. 02NFC29 (2012)

30. Roy, S., Basu, S.: Improved zinc oxide film for gas sensor applications. Bull. Mater. Sci. **25**, 513 (2002)

31. Wang, C., Yin, L., Zhang, L., Xiang, D., Gao, R.: Metal oxide gas sensors: sensitivity and influencing factors. Sensors **10**, 2088 (2010)

32. Sun, Y.F., Liu, S.B., Meng, F.L., Liu, J.Y., Jin, Z., Kong, L.T., Liu, J.H.: Metal oxide nanostructures and their gas sensing properties: a review. Sensors **12**, 2610 (2012)

33. Trakhtenberg, L.I., Gerasimov, G.N., Gromov, V.F., Belysheva, T.V., Ilegbusi, O.J.: Gas semiconducting sensors based on metal oxide nanocomposites. J. Mater. Sci. Res. **1**, 56 (2012)

34. Jiang, X.H., Ma, S.Y., Li, W.Q., Wang, T.T., Jin, W.X., Luo, J., Cheng, L., Mao, Y.Z., Zhang, M.: Synthesis of hierarchical ZnO nanostructure assembled by nanorods and their performance for gas sensing. Mater. Lett. **142**, 299 (2015)

35. Ghobadifard, M., Maleki, Q., Khelghati, M., Zamani, E., Farhadi, S., Aslani, A.: Zinc oxide nano-crystals assisted for carbon dioxide gas sensing prepared by solvothermal and sonochemical methods. Iran. Chem. Commun. **3**, 32 (2015)

36. Mohammed, A.J., Wilde, G.: UTAM ZnO nanostructured thin film CO sensor. In: AMA Conferences, p. 8.8 (2015)

37. Van Quy, N., Minh, V.A., Luan, N.V., Hung, V.N., Hieu, V.H.: Gas sensing properties at room temperature of a quartz crystal microbalance coated with ZnO nanorods. Sens. Actuators B Chem. **153**(1), 188 (2011)

38. Abdul-Hamead, A.A., Osman, F.M., Taeeh, A.S.: Study of ZnO, SnO_2 and compounds ZTO structures synthesized for gas detection. Int. J. Appl. Innov. Eng. Manag. **4**, 140 (2015)